Formulation of stiffness constant and effective mass for a folded beam

Article *in* Archives of Mechanics · January 2010

CITATIONS
63

READS
2,568

3 authors, including:

Wu Wai Chi
Monash University (Australia)
1 PUBLICATION **63** CITATIONS
SEE PROFILE

Burhanuddin Yeop Majlis
National University of Malaysia
532 PUBLICATIONS **4,358** CITATIONS
SEE PROFILE

Arch. Mech., **62**, 5, pp. 405–418, Warszawa 2010

Formulation of stiffness constant and effective mass for a folded beam

W. WAI-CHI[1)], A. A. AZID[1)], B. Y. MAJLIS[2)]

[1)] *School of Mechanical Engineering*
Engineering Campus
Universiti Sains Malaysia
14300 Nibong Tebal
Seberang Perai Selatan, Pulau Pinang, Malaysia
e-mail:

[2)] *Institute of Microengineering and Nanoelectronics*
Universiti Kebangsaan Malaysia
43600 UKM Bangi Selangor, Malaysia

Stiffness constant and effective mass are two important parameters in the performance analysis of an accelerometer. Their values depend mostly on the structural design of the comb finger-type accelerometer, especially its suspension beam design. In this study, the formulation of the stiffness constant and effective mass is derived successfully from theoretical analysis. The performance of the accelerometer can be analyzed using common designs of its suspension beam. The results obtained are comparable with other published results and those obtained from the finite element (FE) analysis.

1. Introduction

Micro-accelerometers or accelerometers are one the most important types of microelectromechanical systems (MEMS) devices, and have generated the second largest sales volume after pressure sensors (Yazdi *et al.* [19]). The large volume demand for MEMS accelerometers is due to multiple applications, such as in measuring tilt, motion, position, vibration and shock). A comb finger-type accelerometer is one of the most important devices used in MEMS due to its high sensitivity and high performance. Comb finger devices can be applied as either MEMS sensors or MEMS actuators. MEMS sensors normally sense the physical environment mechanically or deliver outputs electrically. Comb finger-type sensors have been used in air-bag systems, chassis control, side-impact detection, antilock braking systems, machinery vibration monitoring, inertial navigation, seismology, micro-gravity measurements and mouse applications (Yazdi

et al. [19], Chae *et al.* [4], Amini and Ayazi [1], Xue *et al.* [18]). MEMS actuators respond to electronic commands and actuate dynamic systems. Comb-driven actuators include RF resonators, electromechanical filters, optical MEMS, microgrippers, gyroscopes and voltmeters (Legtenberg *et al.* [8], Yazdi *et al.* [19], Xie *et al.* [17], and Tilleman [13]). They can also drive vibromotors and micromechanical gears (Legtenberg *et al.* [8]).

Stiffness constant and effective mass are two important intermediate parameters in identifying natural frequency and sensitivity. These parameters are determined from a combination of physical and geometrical parameters and material properties, mainly those of the suspension beam. Some common types of suspension beams used in comb finger-type devices include serpentine spring (Luo *et al.* [11], Zhou et al. [21]), folded beam (Borovic *et al.* [3], Chae *et al.* [4], Chae *et al.* [5], Legtenberg *et al.* [8], Liu *et al.* [9], Lüdtke *et al.* [10], Tay *et al.* [12], Zhou *et al.* [20]), crab leg beam (Legtenberg *et al.* [8]), and microbridge (Legtenberg et al. [8], Urey *et al.* [15]).

The commonly used methods in determining stiffness constant and effective mass include finite element (FE) simulation and theoretical derivation. Legtenberg *et al.* [8] and Zhou *et al.* [20] determined the material properties of the suspension beam by using Hooke's law, while stiffness constant is explored by using the total potential energy for several different geometric shapes. Tay *et al.* [12] used Rayleigh's energy principle to detect resonant frequency as a function of effective mass. Wittwer *et al.* [16] used the Castigliano's displacement theorem to analyze vertical deflection due to applied moment or shear force and the geometric shape. In extant literature, only the simplest designs of the suspension beam, such as the cantilever and microbridge, have been derived. Some researchers have identified the stiffness constant of the folded beam, but many assumptions are made merely to simplify the design. Thus, the aim of this study is to formulate equations to determine the stiffness constant and effective mass of the folded beam, taking into account the bending moment and shear effect of the beam. These formulations will enable the researchers to use analytical derivations in order to predict accurately the natural frequencies and sensitivity of the MEMS accelerometer.

In this paper, the stiffness constant of the folded beam in the MEMS accelerometer is verified by using strain energy and the Castigliano's displacement theorem, whereas the effective mass is determined by using the Rayleigh principle. The stiffness constant and effective mass for the folded beam are also identified using a self-developed FE formulation and the ANSYS simulation software. Results with analytical formulation are then compared with results on FE analysis and the previously published results.

2. Design models of suspension beam

A typical design of comb finger-type accelerometer is illustrated in Fig. 1. When the accelerometer is subjected to acceleration, an external force is transferred to the proof mass through the suspension beam. The proof mass, together with movable fingers, moves along and against the forced direction, while the fixed combs remain stationary. This movement changes the capacitance between the fixed fingers and the movable fingers. Capacitance can be measured and calibrated with applied external force. The operations and response of the accelerometer are controlled by the effective mass of movable part (m_e), stiffness constant of suspension beam (k), damping (D) of air surrounding the structure, finger overlap area (A), finger initial sensing gap (d_0), and initial capacitance and acceleration. Among these parameters, k and m_e have the most significant impact on the response of the accelerometer.

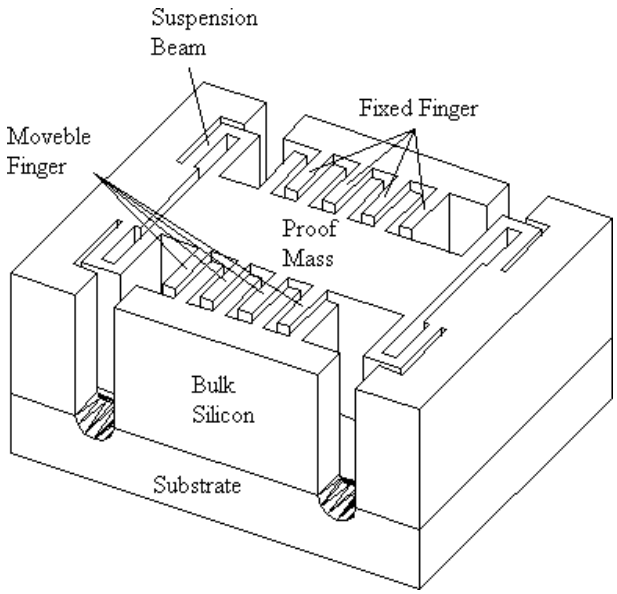

FIG. 1. Typical design of comb finger type accelerometer (LEE *et al.* [7]).

The folded beam, one of the commonly used suspension beam designs of the comb finger-type accelerometer (Fig. 2) is analyzed. A closer view of the folded beam and its corresponding dimension symbols are shown in Fig. 2b. As shown in Fig. 2b, L is the length of the beam, w is the width of the beam, L_{c2} is the length of the second component of the beam, and w_{c2} is the width of the second component of the beam.

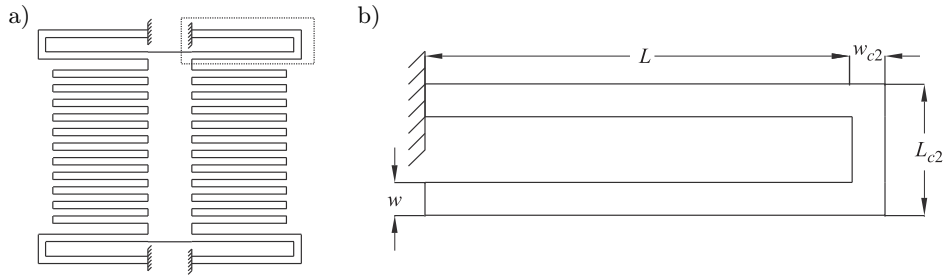

Fig. 2. Folded beam in accelerometer for analysis; a) the device, b) the folded beam.

Most accelerometers are built in consideration of mechanical vibration principles. The principal component of an accelerometer is the proof mass supported by suspension beams, which can be modeled as springs. By referring to Fig. 2a, the proof mass is suspended equally by four beams in four edges. This proof mass can be approximated by a central proof mass suspended by four springs. The free body diagram of a typically arranged accelerometer can be approximated by mass and a spring system, as shown in Fig. 3.

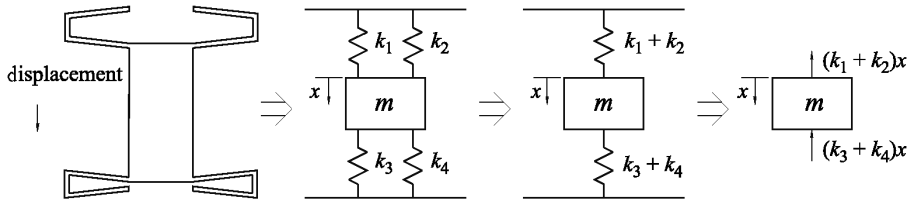

Fig. 3. Free body diagram of typical arrangement of an accelerometer.

In Fig. 3, m is the mass of the proof mass; k_1, k_2, k_3, and k_4 are the stiffness constants of each suspension beam; and x is the displacement. In this spring-mass system, as mass is supported equally by four springs, the external forces are then balanced by the four springs evenly and stored as strain potential energy. The equivalent stiffness constant of the spring mass system, as shown in Fig. 3, can be determined by the equation of equilibrium:

$$\sum F_x = m\ddot{x}, \tag{2.1}$$

$$-(k_1 + k_2)x - (k_3 + k_4)x = m\ddot{x},$$

$$m\ddot{x} + (k_1 + k_2)x + (k_3 + k_4)x = 0,$$

$$m\ddot{x} + (k_1 + k_2 + k_3 + k_4)x = 0,$$

$$m\ddot{x} + k_e x = 0, \tag{2.2}$$

where $\ddot{x}$ is the acceleration and F_x is the force. Therefore, the equilibrium stiffness constant is $k_e = k_1 + k_2 + k_3 + k_4$. Since the four suspension beams are of the same dimensions and materials, then

$$k_1 = k_2 = k_3 = k_4 = k_{1/4} \qquad \text{and} \qquad k_e = 4k_{1/4}, \tag{2.3}$$

where $k_{1/4}$ is the stiffness constant of a quarter system.

3. Analytical derivations

The governing equations of the suspension beam for stiffness constant are derived directly from the internal reactions of bending moment and shear force whenever equilibrium is applied. This derivation is followed by using the superposition method, while the effective mass is determined by using the Rayleigh principle. The following sections describe these derivations.

3.1. Stiffness constant

The resolved components of the folded beam are shown in Fig. 4. The model of the suspension beam together with its boundary condition is shown in Fig. 4a, while its free body diagram is shown in Fig. 4b. In the analysis, the folded beam can be resolved into three components, with two models of half fixed-fixed beams (Figs. 4c and 4d) and a model of bar element (Fig. 4e).

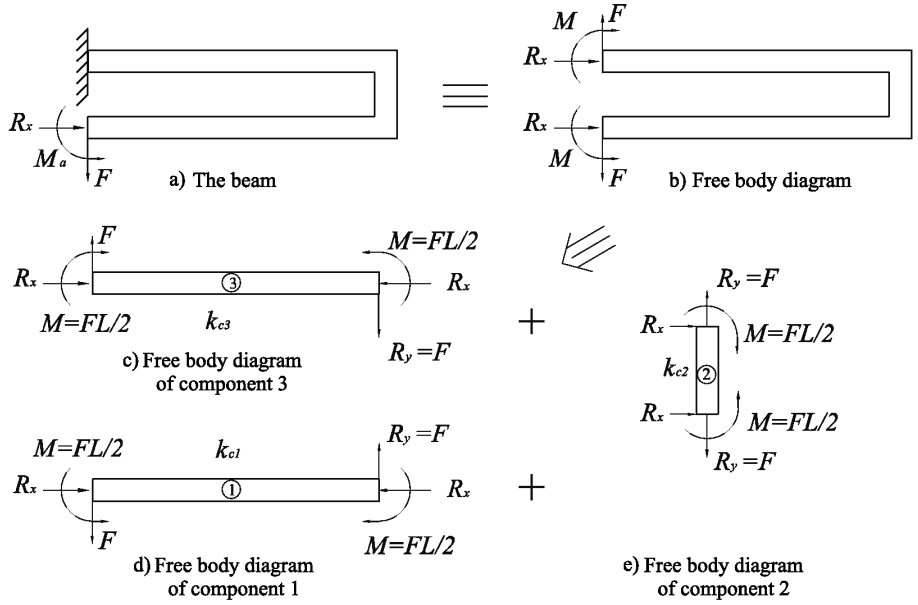

FIG. 4. Resolved components of folded beam.

The folded beam incorporates three components arranged in a series. The stiffness constant of the quarter model can be given in complementary form by

$$\frac{1}{k_{1/4}} = \frac{1}{k_{c1}} + \frac{1}{k_{c2}} + \frac{1}{k_{c3}}. \tag{3.1}$$

a) The stiffness constant for the first and third components

The free body diagram of the first and third components are similar to the model of half fixed-fixed beam subjected to transverse loading, as shown in Fig. 5. Figure 5a shows a fixed-fixed beam with a length ($2L$) under a transverse load (F) at the midspan of the beam. This force causes bending, which resulted in reactions at both fixed ends, consisting of forces and moments. Maximum displacement ($\delta_{\max}$) occurred at the midspan of the beam. If this model is cut through its midspan, this part can be modeled as a half fixed-fixed beam. Figure 5 shows that the reactions at both fixed ends are with bending moment (M_0), shear reaction force in y-direction (R_y), and axial reaction force in x-direction (R_a). As the load is transverse to the axis of the beam, the axial reaction force (R_a) was extremely small compared with the bending moment and shear force. Therefore, R_a was ignored in the calculation. Shear reaction force (R_y) and bending moment (M_0) for the model of a half fixed-fixed beam were obtained as $R_y = F/2$ and $M_0 = FL/4$, respectively.

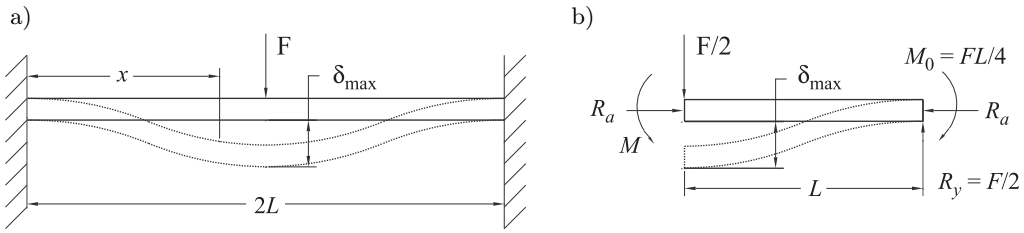

Fig. 5. Fixed-fixed beam; a) fixed-fixed beam under transverse loading F; b) the model of half-fixed beam.

In the model of half fixed-fixed beam, maximum displacement ($\delta_{\max}$) was caused by both the displacements of bending moment (δ_{bm}) and shear (δ_s); for simplification, $\delta_{\max} = \delta_{bm} + \delta_s$. From Hooke's law, $F = k\delta$, so the stiffness is $k = F/\delta_{\max}$; thus, $k \propto 1/\delta_{\max}$. The stiffness constant is normally given by the complementary form, $1/k$. The stiffness constant of the beam is taken as

$$\frac{1}{k_{1c}} = \frac{1}{k_{c3}} = \frac{1}{k_{bm}} + \frac{1}{k_s}. \tag{3.2}$$

The free body diagram of the first and third components were similar to the half model of the fixed-fixed beam.

i) The stiffness constant due to bending moment

For a fixed-fixed beam (Fig. 5), the maximum deflection due to bending moment occurs at the middle of the beam, and is given as

$$\delta_{bm} = \frac{F(2L)^3}{192EI} = \frac{FL^3}{24EI} \qquad \text{(BENHAM [2])}. \tag{3.3}$$

Therefore, the stiffness constant due to bending moment for the full model of the fixed-fixed beam can be expressed as

$$k_{\text{full}} = \frac{F}{\delta_{bm}} = \frac{24EI}{L^3}, \tag{3.4}$$

where E is the Young's modulus and I is the second moment of the cross-sectional area.

For the model of a half fixed-fixed beam, the stiffness constant due to bending moment was one half of the stiffness constant, a result of the bending moment of the fixed-fixed beam. Therefore, the stiffness constant due to bending moment for the half model of a fixed-fixed beam can be derived by

$$k_{bm} = \frac{1}{2}k_{\text{fixed}} = \frac{12EI}{L^3} \tag{3.5}_1$$

or in complementary form, by

$$\frac{1}{k_{bm}} = \frac{L^3}{12EI}. \tag{3.5}_2$$

ii) The stiffness constant due to shear

The stiffness constant due to shear for the first and third components was determined by using the strain energy principle and the equation for shear stress at a point in the transverse section of the beam. For a rectangular cross-section area with specific width (b) and depth (d), total length of beam (L), and applied transverse load ($F/2$), the maximum deflection (at middle point) due to shear is given by

$$\delta_s = \frac{3}{5}\frac{F_s L}{bdG} \qquad \text{(BENHAM [2])}, \tag{3.6}$$

where G is the shear modulus, $G = E/2(1+\mu)$, and μ is the Poison's ratio. Knowing that $F_s = F/2$ and by replacing G and F_s in δ_s, the maximum deflection (at middle point) due to shear can be represented by

$$\delta_s = \frac{6}{5}\frac{(1+\mu)FL}{bdE}. \tag{3.7}$$

As $k_s\delta_s = F$, the stiffness constant due to shear (k_s) is given by

$$\frac{1}{k_s} = \frac{\delta_s}{F} = \frac{6}{5}\frac{(1+\mu)L}{bdE}. \tag{3.8}$$

b) The stiffness constant for the second component

The second component is approximated as a model of a bar element subjected to transverse force and bending moment, transferred from the first and the third components, respectively, as shown in Fig. 4e. This component is subjected to two forces, transverse force (R_y) and bending moment (M). The stiffness constant of the second component (k_{c2}) is a combination of the stiffness constant due to transverse force (k_t) and the stiffness constant due to bending moment (k_m).

i) The stiffness constant due to transverse force

Deflection due to transverse force is expressed as

$$\delta_t = \frac{R_y L_{c2}}{EA_{c2}} = \frac{FL_{c2}}{EA_{c2}}. \tag{3.9}$$

Therefore, the stiffness constant due to transverse force can be solved by

$$\frac{1}{k_t} = \frac{F}{\delta_t} = \frac{L_{c2}}{EA_{c2}}. \tag{3.10}$$

ii) The stiffness constant due to bending moment

Deflection in y direction is given by a previous study (Timoshenko [14]) and expressed as

$$\delta_y = -\frac{ML_{c2}^2}{2EI_{c2}} = -\frac{FLL_{c2}^2}{4EI_{c2}}. \tag{3.11}$$

As $M = FL/2$, the stiffness constant due to bending moment can be given by

$$\frac{1}{k_{bm2}} = \frac{F}{\delta} = -\frac{LL_{c2}^2}{4EI_{c2}}. \tag{3.12}$$

c) The equilibrium stiffness constant of folded beam

The equilibrium stiffness constant of the folded beam can then be determined from Eq. (3.1):

$$\begin{aligned}\frac{1}{k_e} &= \frac{1}{4k_{1/4}} = \frac{1}{4}\left(\frac{1}{k_{1/4}}\right) \\ &= \frac{1}{4}\left(\frac{1}{k_{c1}} + \frac{1}{k_{c2}} + \frac{1}{k_{c3}}\right) = \frac{1}{4k_{c1}} + \frac{1}{4k_{c2}} + \frac{1}{4k_{c3}} \\ &= \frac{1}{4}\left(\frac{1}{k_{bm}} + \frac{1}{k_s}\right) + \frac{1}{4}\left(\frac{1}{k_t} + \frac{1}{k_{bm2}}\right) + \frac{1}{4}\left(\frac{1}{k_{bm}} + \frac{1}{k_s}\right) \\ &= \frac{1}{2k_{bm}} + \frac{1}{2k_s} + \frac{1}{4k_t} + \frac{1}{4k_{bm2}}.\end{aligned} \tag{3.13}$$

The effective stiffness constant of the folded beam can be obtained by substituting Eq. ((3.5)$_2$), Eq. (3.8), Eq. (3.10), and Eq. (3.12) into Eq. (3.13). The resulting equation is

$$\begin{aligned}\frac{1}{k_e} &= \frac{1}{2}\left(\frac{L^3}{12EI}\right) + \frac{1}{2}\left[\frac{6}{5}\frac{(1+\mu)\,L}{bdE}\right] + \frac{1}{4}\left(\frac{L_{c2}}{EA_{c2}}\right) + \frac{1}{4}\left(-\frac{LL_{c2}^2}{4EI_{c2}}\right)\\ &= \frac{L^3}{24EI} + \frac{3}{5}\frac{(1+\mu)\,L}{bdE} + \frac{L_{c2}}{4EA_{c2r}} - \frac{LL_{c2}^2}{16EI_{c2}}\\ &= \frac{1}{Et}\left(\frac{L^3}{2w^3} + \frac{3\,(1+\mu)\,L}{5w} + \frac{L_{c2}}{4w_{c2}} - \frac{3LL_{c2}^2}{4w_{c2}^3}\right).\end{aligned} \tag{3.14}$$

According to the literature, several researchers have determined the stiffness constant of the folded beam. Based on CHAE *et al.* [4], and CHAE *et al.* [5], and BOROVIC *et al.* [3], the stiffness constant of a folded beam can be given by

$$k \approx \frac{24EI}{l_{\text{beam}}^3} = \frac{24E}{l_{\text{beam}}^3} \times \left(\frac{t_{\text{beam}} \cdot w_{\text{beam}}^3}{12}\right), \tag{3.15}$$

where E is the Young's modulus, I is the moment of inertia, and l_{beam} and t_{beam} are the length and thickness of suspension beam, respectively.

Meanwhile, WITTWER *et al.* [16] mentioned that the stiffness constant of the folded beam can be represented by

$$\frac{1}{k_e} = \frac{1}{Et}\left(\frac{L^3}{2w^3} + \frac{6(1+\mu)L}{5w} + \frac{L_r}{2w_r} + \frac{3L^2L_r}{2w_r^3}\right). \tag{3.16}$$

3.2. Effective mass

In addition to the effective stiffness, allowing for the determination of resonant frequency in relation to the bending moment and transverse force, the effective mass also needs to be established. The effective mass of the folded beam was determined by using the Rayleigh principle. By taking the fixed-fixed model with cross-sectional area (A) and length ($2L$), the displacement at any point x is equal to $\delta(x)$ and velocity at any point x is equal to $d\delta(x)/dt$. The displacement at any point ($\delta(x)$) and maximum displacement ($\delta_{\max}$) are related to the distribution function ($N(x)$) as follows:

$$\delta(x) = N(x)\delta_{\max} \qquad \text{and} \qquad \frac{d\delta(x)}{dt} = N(x)\frac{d\delta_{\max}}{dt}. \tag{3.17}$$

Thus, the effective mass can be given by

$$m_e = \rho \int_0^L N^2(x)A(x)dx. \tag{3.18}$$

a) Effective mass for half-model of fixed-fixed beam

As the distribution function is independent of the applied force, the distribution function could be determined by assuming a half-model of the fixed-fixed beam, deflected under a concentrated force (F). Displacement at any point within the beam is given by

$$\delta(x) = \frac{F}{12EI}[3Lx^2 - 2x^3] \qquad \text{(JAMES } et\ al.\text{, [6])}. \tag{3.19}$$

Maximum displacement was observed at the middle of the bridge (i.e., $x = L$). Thus,

$$\delta_{\max} = \frac{FL^3}{12EI}. \tag{3.20}$$

The distribution function is

$$N(x) = \frac{\delta(x)}{\delta_{\max}} = \frac{3Lx^2 - 2x^3}{L^3}. \tag{3.21}$$

The effective mass of the half model of fixed-fixed beam under bending moment was then arrived at by

$$\begin{aligned} m_{b,e} &= \rho \int_0^L N^2(x)A(x)dx = \rho A \int_0^L \left(\frac{3Lx^2 - 2x^3}{L^3}\right)^2 dx \\ &= \frac{\rho A}{L^6}\left[\frac{9L^2x^5}{5} - \frac{12Lx^6}{6} + \frac{4x^7}{7}\right]_0^L = \frac{\rho A}{L^6}\left[\frac{9}{5} - 2 + \frac{4}{7}\right] \times L^7 \\ &= \frac{13}{35}\rho AL. \end{aligned} \tag{3.22}$$

Thus,

$$m_1 = m_3 = m_{b,e} = \frac{13}{35}\rho AL. \tag{3.23}$$

b) Effective mass for second component

For a bar element under transverse force (Fig. 4e), the displacement at any point within the beam can be given by

$$\delta(x) = \frac{x}{L_{c2}}\delta_{\max}. \tag{3.24}$$

The distribution function is

$$N(x) = \frac{\delta(x)}{\delta_{\max}} = \frac{x}{L_{c2}}. \tag{3.25}$$

Thus, the effective mass of bar element under transverse force is

$$m_{t,e} = \rho \int_0^L N^2(x)A(x)dx = \rho A_{c2} \int_0^{L_{c2}} \left(\frac{x}{L_{c2}}\right)^2 dx \tag{3.26}$$
$$= \frac{\rho A_{c2}}{L_{c2}^2}\left[\frac{x^3}{3}\right]_0^{L_{c2}} = \frac{\rho A_{c2}}{L_{c2}^2}\left[\frac{L_{c2}^3}{3}\right]$$
$$= \frac{1}{3}\rho A_{c2} L_{c2}.$$

c) The effective mass of the MEMS accelerometer

The effective mass of the MEMS accelerometer can then be determined by

$$m_e = 8m_{b,e} + 4m_{t,e} + m_{pm} + n\, m_f, \tag{3.27}$$

where m_{pm} is the mass of proof mass, m_f is the mass of finger, and n is the number of fingers.

4. Finite element formulations

The FE formulation of the folded beam for stiffness constant and effective mass were determined by using the MATLAB interface. The frame element formulation was obtained by the combination of beam elements under bending and bar elements under axial loading. The frame element with two nodes per element and three degrees of freedom (DOF) per node was used to formulate the stiffness matrix. MATLAB was also used to simulate the displacement under external load.

5. Finite element modeling with ANSYS

The structural analysis of the accelerometer was conducted by using the FE package, ANSYS (ver. 8.1) simulation software. The simulation result would be used for comparison with the results of the FE analysis using MATLAB and the published results. As the natural frequency and stiffness constant of the accelerometer were the main interest in this analysis, modal analysis and static analysis were employed. The ANSYS BEAM3 software was chosen to run the two-dimensional structural analysis of the folded beam.

6. Results and discussion

In order to compare the applicability of the analytically derived governing equations, the stiffness constant, determined by analytical derivation, was com-

pared with the stiffness constant obtained analytically by Wittwer *et al.* [16] and Chae *et al.* ([4, 5]). In addition, the elastic modulus ($E = 127000$ MPa) was derived for the width and length of the first and third components ($W = 11$ μm and $L = 803$ μm, respectively) and the thickness of device ($t = 120$ μm). A comparative representation of the results obtained by Wittwer *et al.* [16], Chae *et al.* ([4, 5]) with the present study's self-derived analytical solution, FE formulation and ANSYS simulation of the beam model are listed in Table 1. The suspension beam of Designs A, B, and C which have similar basic designs, were analyzed. Design A was with short second component; Design B was wide in the second component; and Design C was long and slender in the second component.

Table 1. Comparative results on stiffness constants obtained from the current study, previous studies (Wittwer, [16]; Chae, [4, 5]), FE formulation, and ANSYS simulation.

Design	l_{c2} (μm)	w_{c2} (μm)	Wittwer [16] Eq. (3.16)	Chae [4, 5] Eq. (3.15)	Current study Eq. (3.14)	FE formulation	ANSYS (Beam model)
A	11	11	75.22	78.35	76.75	76.78	78.43
B	11	55	78.32	78.35	78.33	78.34	82.56
C	100	11	57.02	78.35	66.00	66.63	70.56

From Table 1, it is seen that the stiffness constants solved by using Chae's formula lead to the same result for the three different designs, since this formula has ignored the second component (Fig. 4) in the formulation. Thus, this formula was not applicable for detailed calculation. The stiffness constant solved by using the Wittwer's formula agreed well with the results solved through analytical result formulation and ANSYS for Designs A and B. In the Wittwer's formula, the second component was assumed to be a rigid element, not a frame element; hence, this formula can be only true if the second component is wide or short (e.g., Designs A and B). Both the formulas were applicable, but only under specific conditions, and these limitations were due to the assumptions made on formula derivation.

Both the analytical formula and FE result were in good agreement with the simulation results obtained from ANSYS simulation. The findings proved that the analytical formula can be applied in determining the stiffness constant of the folded beam, as the derivation incorporated all the components of the folded beam.

Both the stiffness constant of the folded beam and the effective mass, as shown by Eq. (3.14) and Eq. (3.27), respectively, can be used to determine the resonant frequency and sensitivity, respectively – these are the two important characteristics of an accelerometer. The resonant frequency (f_r) of the accelerom-

eter with mass (m) is given by the well-known equation,

$$f_r = \frac{1}{2\pi}\sqrt{\frac{k}{m}}. \tag{6.1}$$

Sensitivity can be given in terms of nm/ms^{-2}, which is determined by

$$\text{Sensitivity} = \frac{\text{displacement}}{\text{acceration}} = \frac{\delta}{a} = \frac{m_{\text{eff}}}{k}. \tag{6.2}$$

7. Conclusions

The stiffness constant and effective mass of a folded beam were derived analytically and numerically. The results obtained by these approaches agreed well with the published results. The derived equations were formulated by considering the bending moment and shear effect of the beam. The equations could then be used to predict the natural frequencies and the stiffness constants of accelerometers.

Acknowledgement

This work was carried out under the support of the short-term and the E-science grants, provided by the Universiti Sains Malaysia and the Malaysian Government.

References

1. B.V. Amini, F. Ayazi, *A 2.5V 14-bit ΣΔ CMOS-SOI capacitive accelerometer*, Journal of Solid-State Circuits, **39**, 12, 2467–2476, 2004.
2. P.P. Benham, R.J. Drawford, C.G. Armstrong, *Mechanics of Engineering Materials*, Prentice Hall, Ltd., UK 1996.
3. B. Borovic, A.Q. Liu, D. Popa, H. Cai, F.L. Lewis, *Open-loop versus closed-loop control of MEMS devices: choices and issues*, Journal of Micromechanics and Microengineering, **15**, 1917–1924, 2005.
4. J.S. Chae, H. Kulah, A. Salian, K. Najafi, *A High Sensitivity Silicon on Glass Lateral μg Microaccelerometer*, Third Annual Micro/NanoTechnology Conference, Houston, Texas 2000.
5. J.S. Chae, H. Kulah, K. Najafi, *A hybrid silicon on glass lateral microaccelerometer with CMOS readout circuitry*, Technical Digest, IEEE International Conference on Micro Electro Mechanical Systems, Las Vegas 2002.
6. M.L. James, G.M. Smith, J.C. Wolford, P.W. Whaley, *Vibration of Mechanical and Structural Systems*, Happer and Row Publishers, New York 1989.

7. S.B. Lee, G.J. Nam, J.S. Chae, H.S. Kim, A.J. Drake, *Two-Dimensional Position Detection System with MEMS Accelerometer for MOUSE Applications*, Proceedings of the 38th Design Automation Conference, Las Vegas, USA 2001.

8. R. Legtenberg, A.W. Groeneveld, M. Elwenspoek, *Comb-drive actuators for large displacements*, Journal of Micromechanics and Microengineering, **6**, 320–329, 1996.

9. R. Liu, B. Paden, K. Turner, *MEMS resonators that are robust to process-induced feature width variations*, Journal of Microelectromechanical Systems, **11**, 5, 505–511, 2002.

10. O. Lüdtke, V. Biefeld, A. Buhrdorf, J. Binder, *Laterally driven accelerometer fabricated in single crystalline silicon*, Sensors and Actuators A., **82**, 149–154, 2000.

11. H. Luo, G. Zhang, L.R. Carley, G.K. Fedder, *A post-CMOS micromachined lateral accelerometer*, Journal of Microelectromechanical Systems, **11**, 3, 188–195, 2002.

12. F.E.H. Tay, R. Kumaran, B.L. Chua, V.J. Logeeswaran, *Electrostatic Spring Effect on the Dynamic Performance of Microresonators*, Technical Proceedings of the International Conference on Modeling and Simulation of Microsystems, San Diego, California, USA 2000.

13. M.M. Tilleman, *Analysis of electrostatic comb-driven actuators in linear and nonlinear regions*, International Journal of Solid and Structures, **41**, 4889–4898, 2004.

14. S.P. Timoshenko, J.N. Goodier, *Theory of Elasticity*, 3rd ed., McGraw-Hill Inc, New York, USA 1970.

15. H. Urey, C. Kan, W.O. Davis, *Vibration mode frequency formulae for micromechanical scanners*, Journal of Micromechanics and Microengineering, **15**, 1713–1721, 2005.

16. J.W. Wittwer, L.L. Howell, *Mitigating the effect of local flexibility at the built-in ends of cantilever beams*, Journal of Applied Mechanics, **71**, 748–751, 2004.

17. H.K. Xie, G.K. Fedder, *Vertical comb-finger capacitive actuation and sensing for CMOS-MEMS*, Sensors and Actuators A, **95**, 212–221, 2002.

18. W. Xue, J. Wang, T.H. Cui, *Modeling and design of polymer-based tunneling accelerometers by ANSYS/MATLAB*, IEEE, ASME Transactions on Mechatronics, **10**, 4, 468–472, 2005.

19. N. Yazdi, F. Ayazi, K. Najafi, *Micromachined Inertial Sensors*, Invited Paper, Special Issue of IEEE Proceedings, **86**, 8, 1640–1659, 1998.

20. G.Y. Zhou, P. Dowd, *Tilted folded beam suspension for extending the stable travel range of comb-drive actuators*, Journal of Micromechanics and Microengineering, **13**, 178–183, 2003.

21. N.N. Zhou, A. Agogino, K.S.J. Pister, *Automated Design Synthesis for Micro-Electro-Mechanical Systems (MEMS)*, Proceedings of DETC 2002 on Design Automation, Montreal, Canada 2002.

Received March 12, 2010; revised version June 25, 2010.